Published in final edited form as:
J Am Chem Soc. 2013 April 3; 135(13): 4938–4941. doi:10.1021/ja400836u.

H–H and Si–H Bond Addition to $Fe_{\equiv}NNR_2$ Intermediates Derived from N_2

Daniel L. M. Suess and **Jonas C. Peters***
Division of Chemistry and Chemical Engineering, California Institute of Technology, Pasadena, CA 91125, United States

Abstract

The synthesis and characterization of Fe diphosphineborane complexes are described in the context of N_2 functionalization chemistry. Iron aminoimides can be generated at RT under 1 atm N_2 and are shown to react with E–H bonds from $PhSiH_3$ and H_2. The resulting products derive from delivery of the E fragment to N_α and the H atom to B. The flexibility and lability of the Fe–BPh interactions in these complexes engender this reactivity.

Dinitrogen functionalization reactions using synthetic Fe complexes typically employ reductants in conjunction with electrophilic reagents;[1] this strategy has allowed for the reliable functionalization of N_β in terminal Fe–N_2 complexes (Scheme 1). Whereas early-metal N_2 complexes have displayed rich reactivity with non-polar E–H (E = H, Si) bonds,[2] such reactivity using Fe has little precedent. Addition of H_2 to diiron-bridged nitrides has been demonstrated,[3] and in a recent report the nitrides were derived from reductive cleavage of N_2.[4] The hydrogenolysis of the terminal Fe imide functional group has likewise been established,[5] though these imides were not prepared from N_2. As such, we sought to generate Fe aminoimides from N_2 that could undergo subsequent E–H bond addition across the $Fe_{\equiv}NNR_2$ linkage as a method for N_α functionalization (Scheme 1).

In this context, we and others have studied Fe platforms that can accommodate both N_2 and terminal imide ligands,[1a, 1c, 5a, 6] and we have recently reported that an Fe aminoimide complex **1** (Scheme 2) can be derived from N_2.[1c] Given previous studies that demonstrate H_2 addition across the M–B bonds in related Fe and Ni complexes,[7] we expected that the Fe–B bond in **1** could facilitate an E–H activation step. However, **1** does not react with either H_2 (1 atm) or $PhSiH_3$ at RT. At more elevated temperatures (see SI), **1** decomposes and no tractable products were identified in the presence of H_2 or $PhSiH_3$. We therefore explored the development of a diphosphineborane Fe system ((DPB)Fe) that might be more reactive than the triphosphineborane Fe system ((TPB)Fe) featured in **1**. We now describe new (DPB)$Fe_{\equiv}NNR_2$ complexes that react with non-polar E–H bonds at RT, thereby enabling the one-pot transformation of free N_2 to an Fe hydrazido(−) species—the first such complex to be derived from N_2.

As an entry to useful (DPB)Fe synthons, we found that reductive metallation of isopropyl- and phenyl-substituted DPB ligands[8] **2a** and **2b** (^{iPr}DPB = PhB(*o*-$^{i}Pr_2PC_6H_4)_2$ and ^{Ph}DPB =

Corresponding Author. jpeters@caltech.edu.

ASSOCIATED CONTENT

Supporting Information. Experimental details, spectra, DFT calculations, and XRD tables. This material is available free of charge via the Internet at http://pubs.acs.org.

Funding Sources
No competing financial interests have been declared.

PhB(*o*-$Ph_2PC_6H_4)_2$, respectively, Scheme 3) with $FeBr_2$ and 1.0 equiv Na/Hg in C_6H_6 allows for (DPB)FeBr complexes **3a** and **3b** to be isolated in 84% and 64% yield, respectively. Brown **3a** and **3b** are pseudo-tetrahedral, $S = 3/2$ complexes (μ_{eff} = 3.8 and 3.6 μ_B in C_6D_6 at RT, respectively) that feature η^2-BC interactions that have been previously observed in Cu and Ni complexes of this ligand class.[7,9] The structures determined by XRD analysis (Figure 1 and Table 1; see SI for the XRD structure of **3b**) show close Fe–B (2.3243(11) and 2.330(4) Å, respectively) and Fe–C_{ipso} contacts (2.2605(9) and 2.193(3) Å, respectively), supporting the formulation of the η^2-BC ligand as both a donor *via* a filled π-arene orbital and an acceptor *via* an empty p orbital on boron. In solution, **3a** and **3b** are C_s-symmetric as indicated by their ^{1}H NMR spectra.

Further reduction of **3a** with 1.0 equiv Na/Hg under 1 atm N_2 results in the formation of the dinuclear, bridging N_2 complex ($^{i\text{Pr}}$DPB)Fe(μ-1,2-N_2)Fe($^{i\text{Pr}}$DPB) (**4**). The ^{1}H NMR spectrum of **4** in C_6D_6 indicates that each Fe center is equivalent and has local C_s symmetry. Solution- and solid-state IR spectra of **4** lack an N–N stretch, suggesting that the complex maintains its pseudocentrosymmetric, dinuclear structure in solution. The RT solution magnetic moment is 4.6 μ_B, somewhat higher than the spin-only value of 4.0 μ_B expected for two uncoupled $S = 1$ Fe centers.[10] The two pseudo-tetrahedral Fe centers in **4** have different local geometries in the solid state. The geometry about one of the Fe centers (Fe_A, Figure 1) is distinguished by a short Fe–C_{ortho} contact and relatively long Fe–B and Fe–C_{ispo} distances (Table 1). The other Fe center (Fe_B) displays somewhat shorter Fe–B and Fe–C_{ipso} distances and a negligible Fe–C_{ortho} interaction. The phenyl ring bound to Fe_A exhibits alternating C–C bond lengths (between 1.4303(10) and 1.3711(12) Å; see SI) whereas this asymmetry is negligible for the phenyl ring bound to Fe_B; these metrics indicate that back-donation to the arene ring is more significant for Fe_A and back-donation to the B atom is more significant for Fe_B. Since both (DPB)Fe fragments are equivalent in solution, the Fe–BCC interaction must be highly flexible and the solid-state bond metrics reflect the large range of local geometries available to the Fe centers.

Performing an identical reduction using 1.0 equiv Na/Hg with the phenyl derivative **3b** does not trigger N_2 binding but generates the brown, diamagnetic complex **5** that contains an η^7-BPh interaction; this coordination mode is to our knowledge unprecedented in the metalborane literature. The XRD structure of **5** shows tight Fe–η^7-BPh distances (Figure 2). The bound C_{ipso} atom is significantly pyramidalized as indicated by the sum of the two BCC and one CCC angles (342°). Further showing the significant geometrical distortion of the bound arene is the acute $BC_{ipso}C_{para}$ angle of 127.71(8)°. The η^7-BPh binding mode is maintained in solution based on the significantly upfield-shifted aryl resonances in the ^{1}H NMR spectrum (3.63 (H_{ortho}), 3.24 (H_{meta}), and 6.25 (H_{para}) ppm) and the ^{13}C NMR spectrum (106.77 (C_{ispo}), 99.41 (C_{ortho}), 86.36 (C_{meta}), and 78.73 (C_{para}) ppm).

Each of **3a**, **3b**, **4**, and **5** serves as a precursor to an Fe aminoimide complex derived from N_2. In a nearly identical procedure for generating **1**,[1c] diamagnetic **6a** and **6b** may be accessed by stirring **3a** or **3b** with 1.1 equiv 1,2-bis(chlorodimethylsilyl)ethane and 3.1 equiv Na/Hg in THF under 1 atm N_2. Alternatively, **4** or **5** may be employed as starting materials in conjunction with 2.1 equiv Na/Hg. Both **6a** and **6b** are green in solution and dichroic green/brown when crystalline. The ^{1}H NMR spectrum of **6a** reveals its C_s symmetry in solution. In addition, the ^{1}H resonances of **6a** attributed to the bound aryl ring are shifted upfield (5.10 (H_{ortho}), 6.49 (H_{meta}), and 4.72 (H_{para}) ppm); though this effect is not observed for **6b** perhaps due to attenuated backbonding **6b** due to the less electron-rich metal center.

The solid-state structures of **6a** (Figure 2) and **6b** (see SI) are similar. For **6a**, two molecules are in the asymmetric unit. The short Fe–N distances (1.6607(5) and 1.6657(5) Å for **6a**;

1.6592(7) Å for **6b**) are consistent with other trigonal Fe(NR) linkages and imply an *Fe*≡*N*NR triple bond.[11] The bound arenes display alternating bond lengths that vary between ca. 1.36 and 1.44 Å (see SI). Density functional theory calculations (see SI) support the formulation of **6a** and **6b** as typical pseudotetrahedral d^6 Fe imides[11] that are similar to **1** except that one phosphine donor in **1** has been replaced by the η^3-BCC interaction in **6a** and **6b**. Although the presence of an Fe–B bond is not required for the stability of pseudotetrahedral d^6 Fe imides,[11–12] DFT calculations on **6a**, **1**,[1c] and related Fe imides[6] show some degree of Fe–B σ bonding. Quantifying the extent of Fe–B bonding in these complexes thermodynamically is difficult because the boranes are contained within the cage structures of the ligands.

The reactions of E–H bonds with aminoimides **6a** and **6b** were next examined. We were satisfied to observe that, in contrast to **1**, the room temperature addition of 1.1 equiv $PhSiH_3$ to **6a** readily generates a new, orange species identified as the trisilylhydrazido(−) product **7** resulting from hydrosilylation of the Fe–N bond with delivery of SiH_2Ph to N_α and H to B. To our knowledge, this is the first Fe hydrazido(−) complex to be derived from N_2, thereby adding to the body of previously-reported mononuclear Fe hydrazido(−) model complexes.[13] Having established this elementary step, we sought to combine the formation of **6a** with its subsequent hydrosilylation into a single procedure. Accordingly, **7** may be generated in one pot from **3a** or **4** (eq. 1).

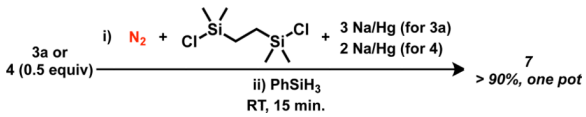

(1)

For complex **7**, an intense IR signal corresponding to the Si–H stretch is observed at 2090 cm^{-1} and a broad, intense IR stretch corresponding to the Fe–H–B functional group is observed at ca. 2000 cm^{-1}. The solution magnetic moment (μ_{eff} = 5.0 μ_B, C_6D_6, RT) indicates an S = 2 spin state. The N–N bond is elongated from 1.326 Å (avg.) in **6a** to 1.492(4) Å in **7** (Figure 3). Although both distances are consistent with N–N single bonds, the comparatively short bond in **6a** is due to the sp hybridization of N_α and some degree of N–N multiple bond character. The very long N–N bond in **7** (longer than that of free N_2H_4) is likely due to a high degree of steric pressure exerted by its bulky Si and Fe substituents. The sum of the CBC angles is 334°, reflecting the tetrahedral geometry of the borohydride ligand.

Addition of 1 atm H_2 at 50 °C to a C_6H_6 solution of **6b** results in a pale brown solution from which colorless solids can be isolated that are identified as the S = 2 product **8** (μ_{eff} = 4.8 μ_B, C_6D_6, RT). Its IR spectrum contains a peak assigned to an N–H stretch at 3343 cm^{-1}; the corresponding D_2 addition product shows $\nu_{(N–D)}$ at 2476 cm^{-1} (2441 cm^{-1} calc.). The broad, intense $\nu_{(Fe–H-B)}$ stretch is observed at ca. 2100 cm^{-1} and is also sensitive to isotopic labeling ($\nu_{(Fe-D–B)} \approx 1550$ cm^{-1}). The connectivity of **8** was established by XRD analysis (Figure 3). In addition to the formation of new N–H and Fe–H–B bonds, the structure of **8** reflects cleavage of the N–N bond, rearrangement of the azadisilacyclopentane ring, and formal oxidation of one of the phosphines. This overall transformation is sufficiently complex that we felt it worthwhile to put forth a tentative mechanism (Scheme 4). The hydrogenation of **6b** to form A is analogous to the formation of **7** from **6a**. The hydrazine rearrangement step to form B has precedent for closely-related disilylhydrazines.[14] Intermediate B may be sufficiently unencumbered to allow for η^2-NN binding to give C which could lead to direct N–N cleavage and group transfer to a phosphine. Alternatively,

the N–N bond in C may be cleaved to form an Fe(IV) imide[15] D which then undergoes group transfer to give **8**. Cleavage of the N–N bond of N_2-derived ligands is rare for Fe[1c, 4] and has been observed for bimetallic early metal complexes.[2h, 16] In addition, the transformation of **6b** to **8** is, to our knowledge, only the second example of N_2 functionalization with H_2 at a well-defined Fe complex.[4]

In conclusion, we have reported the generation of Fe aminoimides from N_2 that undergo subsequent addition of non-polar E–H bonds. The significant flexibility of the Fe–BPh interactions facilitate both the initial formation of the Fe aminoimide as well as the E–H activation step. Whereas previous functionalization reactions of terminal Fe–N_2 fragments allow for derivatization of N_β, this report demonstrates that E–H addition to an unsaturated Fe–N bond is a viable strategy for N_α functionalization.

Supplementary Material

Refer to Web version on PubMed Central for supplementary material.

Acknowledgments

We acknowledge the NIH (GM070757) and the Beckman Institute for funding and thank Lawrence Henling and Dr. Jens Kaiser for assistance with XRD studies. We also acknowledge the Gordon and Betty Moore Foundation, the Beckman Institute, and the Sanofi-Aventis BRP at Caltech for their support of the Molecular Observatory at Caltech. SSRL is operated for the DOE and supported by its Office of Biological and Environmental Research, and by the NIH, NIGMS (including P41GM103393), and the NCRR (P41RR001209).

REFERENCES

1. (a) Betley TA, Peters JC. J. Am. Chem. Soc. 2003; 125:10782–10783. [PubMed: 12952446] (b) Lee Y, Mankad NP, Peters JC. Nature Chemistry. 2010; 2:558–565.(c) Moret M-E, Peters JC. J. Am. Chem. Soc. 2011; 133:18118–18121. [PubMed: 22008018] (d) Yuki M, Tanaka H, Sasaki K, Miyake Y, Yoshizawa K, Nishibayashi Y. Nature Communications. 2012; 3:1254–1256.
2. (a) Fryzuk MD, Love JB, Rettig SJ, Young VG. Science. 1997; 275:1445–1447.(b) Fryzuk MD, MacKay BA, Patrick BO. J. Am. Chem. Soc. 2003; 125:3234–3235. [PubMed: 12630877] (c) Pool JA, Lobkovsky E, Chirik PJ. Nature. 2004; 427:527–530. [PubMed: 14765191] (d) Pool JA, Bernskoetter WH, Chirik PJ. J. Am. Chem. Soc. 2004; 126:14326–14327. [PubMed: 15521731] (e) Hirotsu M, Fontaine PP, Epshteyn A, Sita LR. J. Am. Chem. Soc. 2007; 129:9284–9285. [PubMed: 17625853] (f) Hirotsu M, Fontaine PP, Zavalij PY, Sita LR. J. Am. Chem. Soc. 2007; 129:12690–12692. [PubMed: 17902670] (g) Pun D, Bradley CA, Lobkovsky E, Keresztes I, Chirik PJ. J. Am. Chem. Soc. 2008; 130:14046–14047. [PubMed: 18826309] (h) Semproni SP, Lobkovsky E, Chirik PJ. J. Am. Chem. Soc. 2011; 133:10406–10409. [PubMed: 21682285]
3. Brown SD, Mehn MP, Peters JC. J. Am. Chem. Soc. 2005; 127:13146–13147. [PubMed: 16173733]
4. Rodriguez MM, Bill E, Brennessel WW, Holland PL. Science. 2011; 334:780–783. [PubMed: 22076372]
5. (a) Brown SD, Peters JC. J. Am. Chem. Soc. 2004; 126:4538–4539. [PubMed: 15070370] (b) Bart SC, Lobkovsky E, Bill E, Chirik PJ. J. Am. Chem. Soc. 2006; 128:5302–5303. [PubMed: 16620076]
6. Moret M-E, Peters JC. Angew. Chem. Int. Ed. 2011; 50:2063–2067.
7. (a) Harman WH, Peters JC. J. Am. Chem. Soc. 2012; 134:5080–5082. [PubMed: 22380492] (b) Fong H, Moret M-E, Lee Y, Peters JC. *submitted*.
8. (a) Bontemps S, Gornitzka H, Bouhadir G, Miqueu K, Bourissou D. Angew. Chem. Int. Ed. 2006; 45:1611–1614.(b) Sircoglou M, Bontemps S, Mercy M, Saffon N, Takahashi M, Bouhadir G, Maron L, Bourissou D. Angew. Chem. Int. Ed. 2007; 46:8583–8586.
9. (a) Emslie DJH, Cowie BE, Kolpin KB. Dalton Trans. 2012; 41:1101. [PubMed: 21983808] (b) Sircoglou M, Bontemps S, Mercy M, Miqueu K, Ladeira S, Saffon N, Maron L, Bouhadir G, Bourissou D. Inorg. Chem. 2010; 49:3983–3990. [PubMed: 19891437]

10. (a) Smith JM, Lachicotte RJ, Pittard KA, Cundari TR, Lukat-Rodgers G, Rodgers KR, Holland PL. J. Am. Chem. Soc. 2001; 123:9222–9223. [PubMed: 11552855] (b) Hendrich MP, Gunderson W, Behan RK, Green MT, Mehn MP, Betley TA, Lu CC, Peters JC. Proc. Natl. Acad. Sci. U.S.A. 2006; 103:17107–17112. [PubMed: 17090681] (c) Field LD, Guest RW, Turner P. Inorg. Chem. 2010; 49:9086–9093. [PubMed: 20815362]
11. Saouma CT, Peters JC. Coordination Chemistry Reviews. 2011; 255:920–937. [PubMed: 21625302]
12. Brown SD, Peters JC. J. Am. Chem. Soc. 2005; 127:1913–1923. [PubMed: 15701026]
13. Selected examples: Smith JM, Lachicotte RJ, Holland PL. J. Am. Chem. Soc. 2003; 125:15752–15753. [PubMed: 14677959] Crossland JL, Balesdent CG, Tyler DR. Dalton Trans. 2009:4420. [PubMed: 19488434] Saouma CT, Kinney RA, Hoffman BM, Peters JC. Angew. Chem. Int. Ed. 2011; 50:3446–3449.
14. Pitt CG, Skillern KR. Inorganic and Nuclear Chemistry Letters. 1966; 2:237–241.
15. Thomas CM, Mankad NP, Peters JC. J. Am. Chem. Soc. 2006; 128:4956–4957. [PubMed: 16608321]
16. Selected examples: Peters JC, Cherry J-PF, Thomas JC, Baraldo L, Mindiola DJ, Davis WM, Cummins CC. J. Am. Chem. Soc. 1999; 121:10053–10067. Fryzuk MD. Acc. Chem. Res. 2009; 42:127–133. [PubMed: 18803409] Knobloch DJ, Lobkovsky E, Chirik PJ. Nature Chemistry. 2009; 2:30–35. Knobloch DJ, Lobkovsky E, Chirik PJ. J. Am. Chem. Soc. 2010; 132:10553–10564. [PubMed: 20662528]

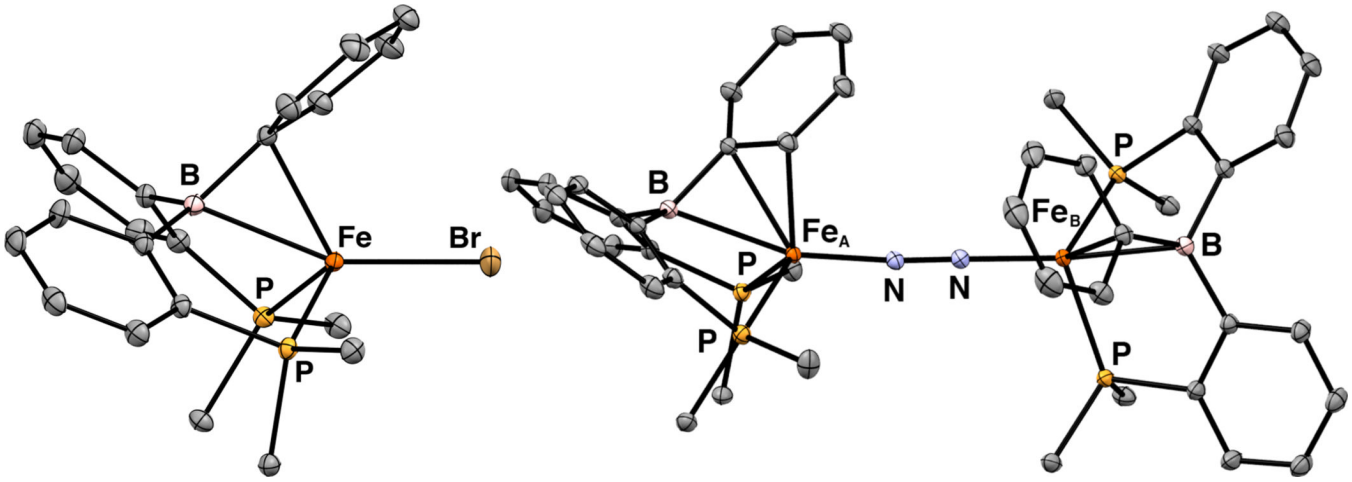

Figure 1.
Displacement ellipsoid (50%) representations of **3a** (left) and **4** (right). P^{i}Pr$_2$ groups are truncated and H atoms are omitted for clarity.

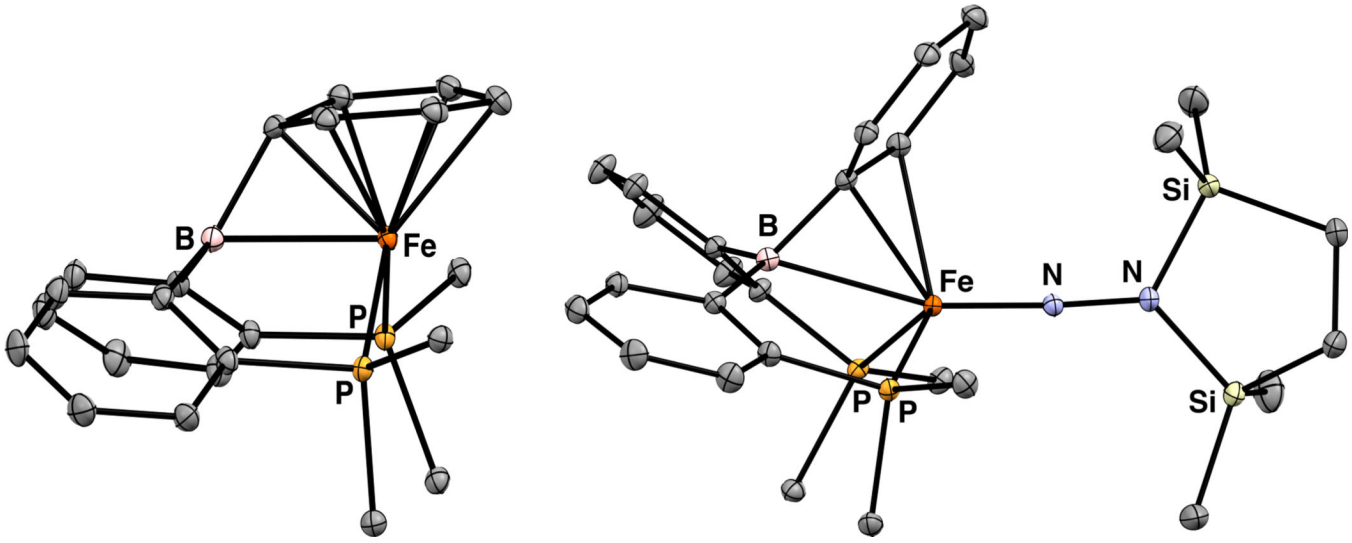

Figure 2.

Displacement ellipsoid (50%) representations of **5** (left) and **6a** (right). PR_2 groups are truncated. H atoms and solvent molecules are omitted for clarity. For **6a**: Only one of the two molecules per asymmetric unit is shown. Selected distances (Å) for **5**: Fe–B = 2.2667(13), Fe–C_{ipso} = 1.9669(11), Fe–C_{ortho} = 2.090 (avg), Fe–C_{meta} = 2.169 (avg), Fe–C_{para} = 2.1933(11).

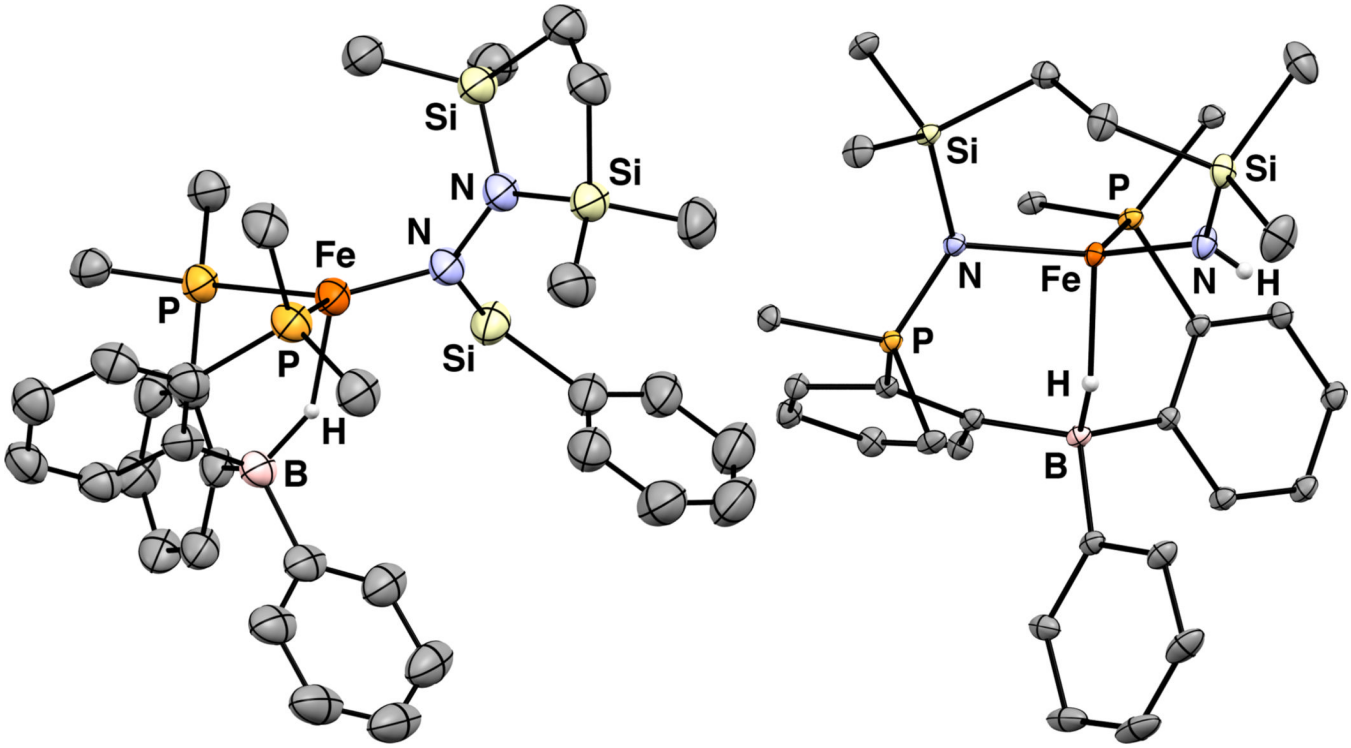

Figure 3.
Displacement ellipsoid (50%) representation of **7** (left) and **8** (right). PR_2 groups are truncated. H atoms not located in the difference map and solvent molecules are omitted for clarity.

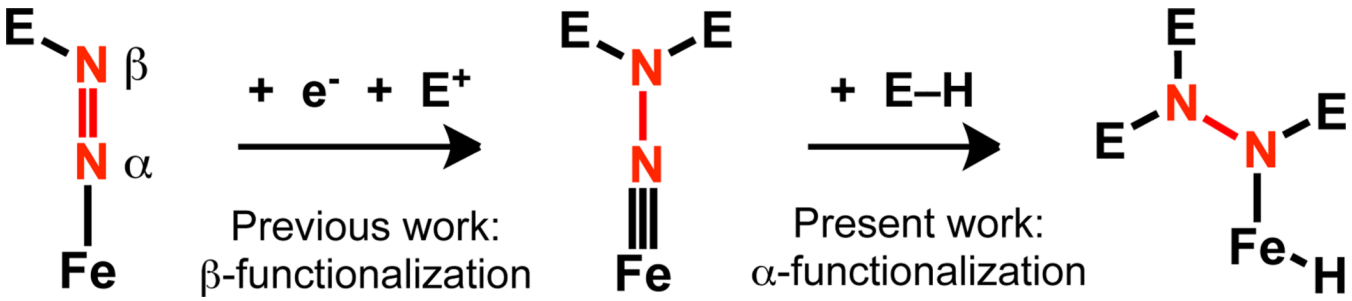

Scheme 1.

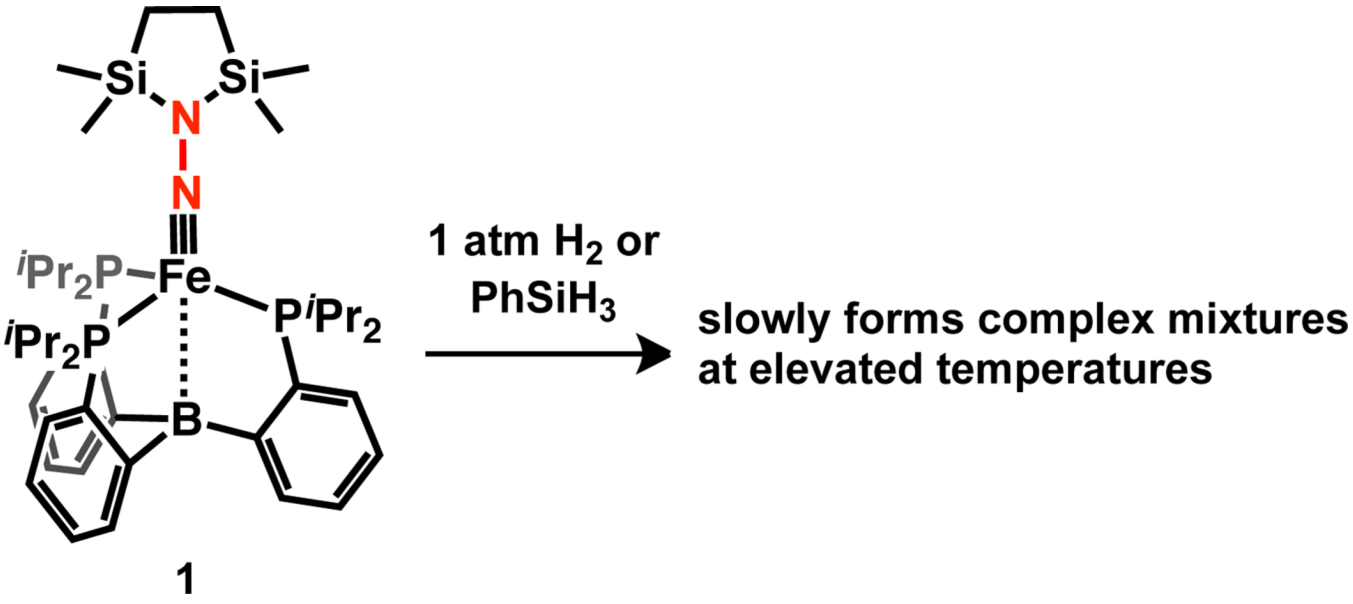

Scheme 2.

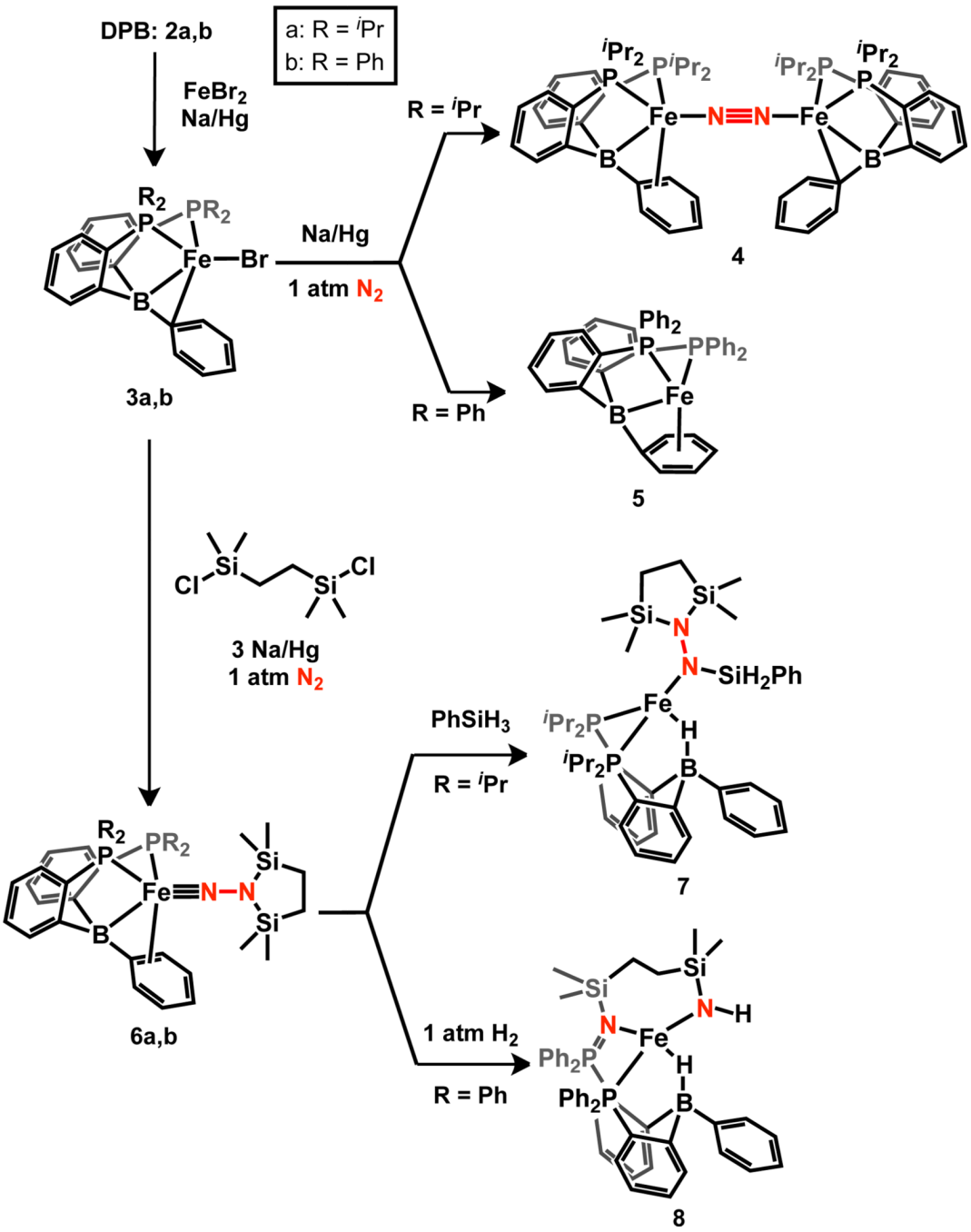

Scheme 3.

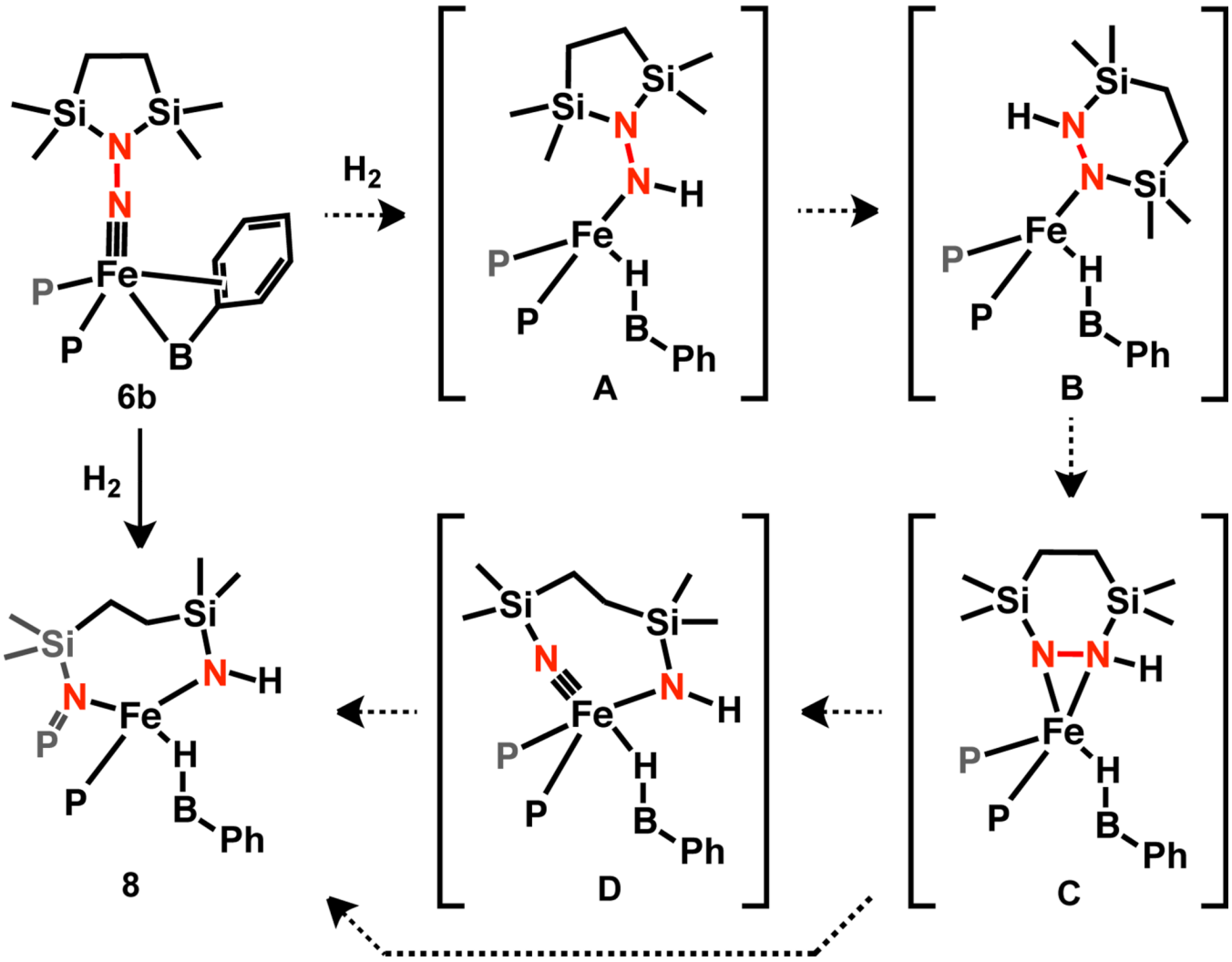

Scheme 4.

Table 1

Selected bond lengths (Å)

	Fe–B	Fe–C_{ipso}	Fe–C_{ortho}
3a	2.3242(11)	2.2605(9)	2.5483(11)
4: Fe_A [a]	2.3739(7)	2.2516(6)	2.2714(7)
4: Fe_B [a]	2.3136(7)	2.2133(6)	2.6642(7)
6a[b]	2.3768(6)	2.1492(5)	2.3403(6)
	2.4288(7)	2.1440(6)	2.2266(6)
7	2.859(5)	-	-

[a] Two unique Fe atoms per molecule.

[b] Two molecules per asymmetric unit.